

Screening in the two-dimensional electron gas with spin-orbit coupling

M. Pletyukhov¹ and V. Gritsev^{2,3}

¹*Institut für Theoretische Festkörperphysik, Universität Karlsruhe, D-76128 Karlsruhe, Germany*

²*Département de Physique, Université de Fribourg, CH-1700 Fribourg, Switzerland*

³*Department of Physics, Harvard University, Cambridge, MA 02138, USA*

We study the interplay between electron-electron interaction and Rashba spin-orbit coupling in the two-dimensional electron gas. Using the random phase approximation we predict new screening properties of the electron gas which result in extension of the region of particle-hole excitations and in spin-orbit induced suppression of collective modes. In particular, we observe that the spin-orbit coupling gives a finite lifetime to plasmons and longitudinal optical phonons, which can be resolved in inelastic Raman scattering. We evaluate the experimentally measurable dynamic structure factor and estimate the range of parameters where the described phenomena are mostly pronounced.

PACS numbers: 71.70.Ej, 73.20.Mf, 73.21.-b

Fundamental issues of interaction effects in the two-dimensional electron gas (2DEG) are at the center of discussions since the early days of its fabrication [1]. Quite generally, screening described by the dielectric function forms the basis for understanding a variety of static and dynamic many-body effects in electron systems [2]. The dielectric function of the 2DEG was computed a long time ago by F. Stern [3] within the random phase approximation (RPA). Different quasiparticle and collective (plasma) properties deduced from these expressions were confirmed experimentally soon after [4]. Recent experiments measuring plasmon dispersion, retardation effects and damping [5, 6, 7] unambiguously show the importance of correlations between electrons.

More recently, the possibility of manipulating spin in 2DEG by nonmagnetic means has generated a lot of activity [8]. The key ingredient is spin-orbit (SO) coupling tunable by an applied electric field [9]. A recent example for SO-induced phenomena is the spin-Hall effect [10].

In this context understanding of the combined effects of electron-electron correlations and SO coupling in 2DEG becomes vitally important. In the present paper we study the RPA dielectric function at finite momenta and frequencies treating the SO coupling exactly. We observe two interesting phenomena: an extension of the continuum of particle-hole excitations and SO-induced damping of collective modes. New features in the dynamic structure factor are predicted, and SO-induced widths of both plasmon and longitudinal optical phonon spectra are evaluated. Their values lie in the ranges which are experimentally accessible by now in the inelastic Raman scattering measurements. We also revisit the derivation of zero-frequency limit of the dielectric function and present an analytic result which does not contain an anomaly at small momenta [11].

We consider a 2DEG with SO coupling of the Rashba type [12] described by the single-particle Hamiltonian $H = \frac{\mathbf{k}^2}{2m^*} + \alpha_R \mathbf{n}(\boldsymbol{\sigma} \times \mathbf{k})$, where \mathbf{n} is a unit vector normal to the plane of 2DEG and $\hbar = 1$. The dispersion relation is SO-split into two subbands $\epsilon_{\mathbf{k}}^{\pm} = \frac{k^2}{2m^*} \pm \alpha_R k$ with two

distinct Fermi momenta $k_{\pm} = k_F \mp m^* \alpha_R \equiv k_F \mp k_R$, but with the same Fermi velocity $v_F = k_F/m^*$. The effective Coulomb interaction is $V_{q\omega}^{eff} = V_q/\epsilon_{q\omega}$, where $V_q = 2\pi e^2/(q\epsilon_{\infty})$, ϵ_{∞} is the (high-frequency) dielectric constant of medium, and the dielectric function $\epsilon_{q\omega} = \epsilon_{1,q\omega} + i\epsilon_{2,q\omega}$ describes effects of dynamic screening. In RPA, $\epsilon_{q\omega} = 1 - V_q \Pi_{q\omega}$, where $\Pi_{q\omega}$ is the polarization operator. In the presence of SO coupling $\Pi_{q\omega} = \Pi_{q\omega}^+ + \Pi_{q\omega}^-$ includes contributions from intersubband (+) and intra-subband (-) transitions:

$$\Pi_{q\omega}^{\pm} = \lim_{\delta \rightarrow 0} \sum_{\mu=\pm} \int \frac{d^2\mathbf{k}}{(2\pi)^2} \frac{n_F(\epsilon_{\mathbf{k}}^{\mu}) - n_F(\epsilon_{\mathbf{k}+\mathbf{q}}^{\pm\mu})}{\omega + i\delta + \epsilon_{\mathbf{k}}^{\mu} - \epsilon_{\mathbf{k}+\mathbf{q}}^{\pm\mu}} \mathcal{F}_{\mathbf{k},\mathbf{k}+\mathbf{q}}^{\pm} \quad (1)$$

where the form factors $\mathcal{F}_{\mathbf{k},\mathbf{k}+\mathbf{q}}^{\pm} = \frac{1}{2}[1 \pm \cos(\phi_{\mathbf{k}} - \phi_{\mathbf{k}+\mathbf{q}})]$ originate from the rotation to the eigenvector basis.

We now discuss our results for $\epsilon_{q\omega}^{RPA}$. We have derived them in the analytic form which will be presented in a subsequent paper. Here we discuss the main SO-induced effects for the range of small z and w , and describe how they depend on the SO-coupling strength $y = k_R/k_F$ and on the Wigner-Seitz parameter $r_s = 1/\sqrt{n\pi a_B^*}$ which is defined by an electron density n and effective Bohr radius $a_B^* = \epsilon_{\infty} m_e a_B/m^*$. Our main results are compactly summarized in Fig. 1 which shows the contour plots and cross sections of the structure factor $S(z, w) = -\text{Im}[1/\epsilon(z, w)]$ for different values of y and r_s . The introduced notations $z = q/2k_F$ and $w = m^* \omega/2k_F^2$, are, respectively, the dimensionless wave vector and frequency.

First of all, we observe an extension of the continuum of particle-hole excitations (or Landau damping region) defined by $\epsilon_2 \neq 0$. A new wedge-shaped region of damping is generated by the SO coupling. It is bounded by two parabolas $-(z-y)^2 - (z-y) < w < (z+y)^2 + (z+y)$ (black-dashed lines in Fig. 1) and attached to the boundary $w = z^2 + z$ (white-dashed line in Fig. 1) of the conventional particle-hole continuum (obtained in the absence of SO coupling according to [3]). Another boundary $w = z^2 - z$ of the latter transforms

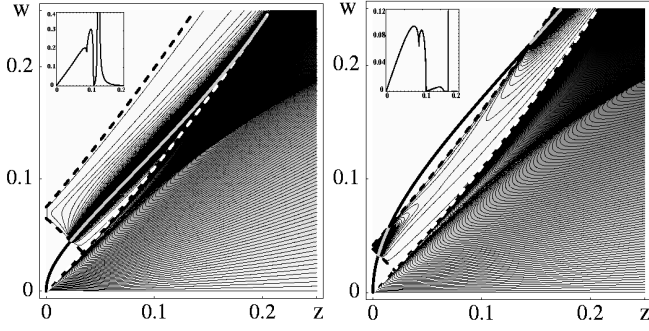


FIG. 1: Contour plots of $S(z, w)$ showing the SO-induced wedge-shaped damping region (bounded by the dashed lines). The plasmon mode is depicted by the bold line. Insets show the cross-sections $S(z = 0.1, w)$ as a function of w . *Left panel:* $y = 0.07$, $r_s = 0.2$. *Right panel:* $y = 0.04$, $r_s = 0.6$.

into $w = (z - y)^2 - (z - y)$ for nonzero y (this occurs at $z > 1$ which are not shown in Fig. 1). The new regions of damping reflect an opened possibility for transitions between SO-split subbands, and $S(z, w)$ strongly depends on y inside these regions. Their boundaries can be determined from a simple consideration of extremes of the denominators in (1). On the other hand, within the conventional boundaries $w = z^2 \pm z$ the function $S(z, w)$ is modified by SO coupling only slightly and can be approximated by Stern's expressions [3].

The second SO-induced modification is the broadening of a plasmon collective mode within the new particle-hole continuum. We determine numerically the position of the plasmon spectrum from the equation $\varepsilon_1(z, w) = 0$ and depict it in Fig. 1 by the bold line, in black where $\varepsilon_2 = 0$ (undamped plasmon, the structure factor is delta-peaked) and in gray where $\varepsilon_2 \neq 0$ (SO-damped plasmon, the structure factor has finite height and width). Two different cases are possible: (I) the plasmon enters only once into the SO-induced damping region (Fig. 1, left panel); (II) it enters twice escaping for a while after the first entrance (Fig. 1, right panel). We observe that the position of the plasmon in the presence of SO coupling is almost indistinguishable (at least, on the scale of Fig. 1) from the RPA result derived in the absence of SO coupling [13]

$$w_{pl}(z) = \frac{z(z + 2\tilde{r}_s)}{2\tilde{r}_s} \sqrt{\frac{4\tilde{r}_s^2 + 4\tilde{r}_s z^3 + z^4}{z(z + 4\tilde{r}_s)}} \Theta(z^* - z), \quad (2)$$

where $\tilde{r}_s = r_s/\sqrt{8}$ and z^* is the real positive root of the equation $z^2(z + 4\tilde{r}_s) = 4\tilde{r}_s^2$. Later we will comment more on how small might be the difference between the exact SO-modified plasmon dispersion and that given by (2). At the moment we will use (2) in order to calculate critical values of y and r_s which separate the cases (I) and (II). The result is represented in Fig. 2 where the plane (y, r_s) is divided into the respective domains I and II. Changing y and r_s , we can tune the relative position

of the new particle-hole region and $w_{pl}(z)$.

In the new region of damping the dynamic structure factor is very well approximated by the Lorentzian

$$S(z, w)_{SO-damp pl} = \frac{\alpha(z)}{\pi} \frac{\gamma(z)}{(w - w_{pl}(z))^2 + \gamma^2(z)}, \quad (3)$$

which describes the SO-damped plasmon with the width $\gamma(z)$. The weight factor $\alpha(z) = \pi(d\varepsilon_1/dw|_{w=w_{pl}(z)})^{-1}$ is practically independent of y and given by its value at $y = 0$

$$\alpha(z) = \frac{\pi\sqrt{z}[16\tilde{r}_s^4 - z^4(z + 4\tilde{r}_s)^2]}{2\tilde{r}_s\sqrt{(4\tilde{r}_s^2 + 4\tilde{r}_s z^3 + z^4)(z + 4\tilde{r}_s)^3}}. \quad (4)$$

At the same time, the SO-induced width $\gamma(z) = \alpha(z)\varepsilon_2(z, w_{pl}(z))/\pi$ strongly depends on y via $\varepsilon_2 \neq 0$. The insets in Fig. 2 show $\bar{\gamma}(z) = \gamma(z) \times 10^4$ for the values of parameters same as in Fig. 1: (I) $y = 0.07$, $r_s = 0.2$; (II) $y = 0.04$, $r_s = 0.6$. The function $\gamma(z)$ is defined for $z \leq z^*$ and vanishes in the region where the plasmon is undamped. In the latter case $S(z, w)_{pl} = \alpha(z)\delta(w - w_{pl}(z))$.

Comparing positions of peaks in constant- z cross-sections of the exact $S(z, w)$ and of the approximate $S(z, w)_{SO-damp pl}$ (3), we have observed that the shift of the plasmon dispersion due to SO coupling from $w_{pl}(z)$ (2) is one or two orders of magnitude smaller than $\gamma(z)$ (unless $\gamma(z) = 0$), and therefore can hardly be resolved experimentally.

It is also worthwhile to compare our exact results with an approximation commonly used in the literature. It is based on the formula $\Pi_{q\omega} \approx -i\sigma_\omega q^2/(e^2\omega)$ for small q , where σ_ω is the ac conductivity (cf., e.g., Refs. [14, 15, 16]). Such approximation takes into account only the transitions with zero momentum transfer,

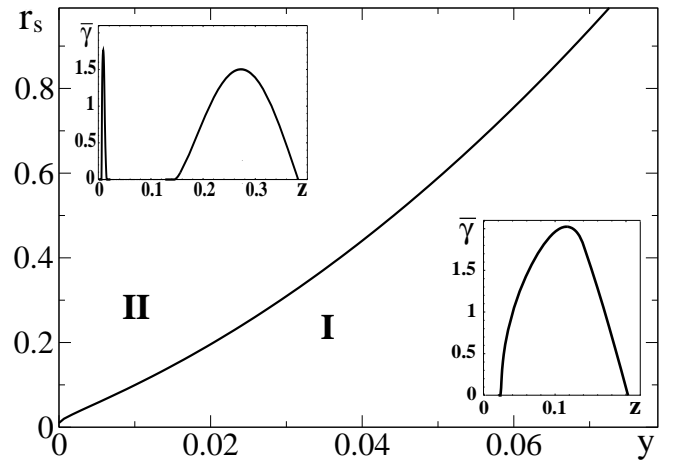


FIG. 2: The plane (y, r_s) is divided into the domains I and II where the plasmon has one or two undamped pieces, respectively (cf. Fig. 1). Insets show SO-induced plasmon width $\bar{\gamma}(z) = \gamma(z) \times 10^4$ for the same parameters as in Fig. 1.

and therefore leads to the kinematic extension of the conventional particle-hole continuum to a strip $y - y^2 < w < y + y^2$ parallel to the z -axis. The lines $w = y \pm y^2$ coincide with the parabolas $w = \pm(z \pm y)^2 \pm (z \pm y)$ at $z = 0$ only, i.e. where the above relation between $\Pi_{q\omega}$ and σ_ω becomes exact. This approximation can be justified for very small momenta (e.g., up to $z \approx 10^{-5}$ for $y = 0.01$ and up to $z \approx 10^{-7}$ for $y = 0.001$). However, it fails to describe properly the behavior of the plasmon mode at larger z . For example, according to [14] the plasmon spectrum does not cross the border of their damping region but rather approaches it exponentially from

$$-\frac{2\pi}{m^*}\Pi_1(z, 0) = 2\Theta(1 - y - z) + \Theta(y - |z - 1|) \left(1 + \frac{\pi}{2}\sin\psi\right) - 2\Theta(z - 1)\operatorname{arccosh}z \cos\psi + \sum_{\nu=\pm} \Theta(z - (1 + \nu y)) \left(1 + \nu\psi_\nu \sin\psi - \cos\psi_\nu - 2\cos\psi \ln \frac{1 + z \sin(\psi_\nu - \nu\psi)}{2\sqrt{2z} \cos \frac{1}{2}\psi_\nu \cos \frac{1}{2}\psi}\right), \quad (5)$$

where $\sin\psi = y/z \leq 1$ and $\sin\psi_\nu = (1 + \nu y)/z \leq 1$ are defined in the corresponding ranges of z restricted by the unit-step function Θ . It is assumed that $y < 1/2$ (or $2k_R < k_F$). For the values $z \leq 1 - y$ the expression (5) yields $-\Pi_1(z, 0) = m^*/\pi$, the density of states in 2DEG. In deriving $\Pi_1(z, 0)$ we first perform the momentum integration in (1), and only then take the limit $\delta \rightarrow 0$. Once this sequence is reversed, there would arise the extra term $-\pi\Theta(y - z)\sqrt{(y/z)^2 - 1}$ in the rhs of (5), which produces an anomaly at $z = y$ (cf. Ref. [11]).

The effect of SO-induced plasmon broadening described above can be observed experimentally. For instance, one can directly measure $S(z, w)$ by means of inelastic light (Raman) scattering (see, e.g., [17]). Keeping z at a fixed value and varying y and r_s , one should observe different patterns with either damped or undamped plasmon, like those shown in the insets to Fig. 1 where the sections of $S(z, w)$ at constant $z = 0.1$ are presented. In order to estimate realistic parameters we focus on InAs-based 2DEG where the strength of Rashba coupling α_R has quite large values up to $\sim 3 \times 10^{-11}$ eVm [18] and prevails over the Dresselhaus term [19]. Most of experiments deal with the 2DEG's densities ranging from $n = 0.7 \times 10^{16}$ m $^{-2}$ [20] to $n = 2.4 \times 10^{16}$ m $^{-2}$ [9]. Taking $\varepsilon_\infty \approx 12$ and $m^* \approx 0.03m_e$ we obtain the range of y from 0.04 to 0.075 and the range of r_s from 0.38 to 0.3. These values belong to the domain I in Fig. 2 where the SO-damping of the plasmon is especially important. Choosing the value of $\gamma \sim 10^{-4}$, we establish that $2\tau_{pl} = \hbar/(4\gamma\varepsilon_F)$ is of the order of 10 ps. This can, in principle, be resolved experimentally, since the Raman measurements done in II-VI quantum wells [21] give a finite lifetime of the plasmon mode with the typical value

both sides of the strip. This approximation also misses the possibility, shown in the left panel of Fig. 1, that the plasmon does not emerge undamped for intermediate momenta.

An important test of our results is provided by the Kramers-Kronig relations and the sum rules. In particular, we have checked numerically that our expressions for $\varepsilon(z, w) - 1$ and $1/\varepsilon(z, w) - 1$ both satisfy the zero-frequency Kramers-Kronig relations, which link $\varepsilon_2(z, w)$ and $S(z, w)$ to the static dielectric function $\varepsilon_1(z, 0) = 1 - (\tilde{r}_s/z) \cdot (2\pi\Pi_1(z, 0)/m^*)$. Our exact result for zero-frequency polarization operator is

$2\tau_{pl} \sim 0.3$ ps.

Plasmon broadening may be also caused by thermal effects. We use the results for 2DEG at finite temperature [22] in order to estimate the relative contributions of SO-induced and thermal damping. The former dominates over the latter below some characteristic temperature which is about 90 K for the parameters of Ref. [18]. This estimate is made at constant $z = 0.1$. Note that the thermal damping strongly depends on the values of r_s and temperature whereas the SO-induced damping has quite a weak r_s -dependence (e.g., compare the insets in Fig. 2). This may provide a guide for an experimental separation of these two sources of broadening.

Our result for the dynamic structure factor indicates that the other collective mode, longitudinal optical (LO) phonon, will also experience a pronounced SO-induced damping. Its dispersion and lifetime can be obtained from the renormalized propagator which is expressed in RPA as [23]

$$D(q, \omega) = \frac{2\omega_{LO}}{\omega^2 - \omega_{LO}^2 - 2\omega_{LO}M_q^2\Pi_{q\omega}/\varepsilon_{q\omega}}, \quad (6)$$

where $M_q^2 = \frac{1}{2}A\omega_{LO}V_q$, and $A = 1 - \varepsilon_\infty/\varepsilon_0$. On the basis of this expression we can establish that the LO-phonon width (normalized by $2k_F^2/m^*$) equals

$$\gamma_{LO}(z) = \frac{AS(z, w)w_0^2\varepsilon_1^2}{2w\varepsilon_1^2 + Aw_0^2(\partial\varepsilon_1/\partial w)} \Big|_{w=w_{ph}(z)}, \quad (7)$$

where $w_0 = (m^*/2k_F^2)\omega_{LO}$ and $w_{ph}(z)$ is the renormalized phonon spectrum. Like in the case of plasmons, we may neglect the dependence of $w_{ph}(z)$ on SO coupling, and find the phonon spectrum from the equation $w^2 = w_0^2[1 + A(1/\varepsilon_1 - 1)]$, where ε_1 is taken at $y = 0$.

The lifetime effects of the LO phonons can be very important for a coupled dynamics of carriers and phonons. An interesting possibility arises when $\omega_{LO} \sim 2\alpha_R k_F$ (or $w_0 \sim y$). This, for example, holds in InAs, where the value $\omega_{LO} \approx 28$ meV gives $w_0 \approx 0.07$. Changing the Rashba coupling strength α_R by an applied electric field one can manipulate the lifetime of an optical phonon which would result in a modification of transport properties by virtue of the electron-phonon coupling.

In Fig. 3 we show the function $\bar{\gamma}_{LO}(z) = \gamma_{LO}(z) \times 10^4$. In our calculations we used the following parameters: $w_0 = 0.07$, $r_s = 0.4$, $\varepsilon_\infty = 12$ and $\varepsilon_0 = 15$ (for InAs). Choosing the value $\gamma_{LO} = 10^{-4}$ we find that for LO phonons the SO-induced lifetime $2\tau_{LO}$ is of the order of 10 ps as well. We note that the typical lifetime for the LO phonons measured in AlAs and GaAs by the Raman spectroscopy is of the same order [24]. One can observe that for $y = 0.07$ ($|w_0 - y| < y^2$) the damping is always finite (solid line), while for $y = 0.06$ ($|w_0 - y| > y^2$) it becomes nonzero only after some value $z \approx 0.007$ (dashed line). In the two insets we show the relative location of the phonon spectrum (solid line) and of the SO-induced damping region (dashed lines). We also depict the boundaries of the strip $w = y \pm y^2$ (dotted lines), and one can see that for $y = 0.07$ the phonon spectrum leaves it at the value $z \approx 0.017$ (left inset), while for $y = 0.06$ the phonon spectrum never gets inside the strip (right inset).

In conclusion, we have calculated the dielectric function of 2DEG with Rashba spin-orbit coupling in RPA. We have found that the spin-orbit coupling leads to

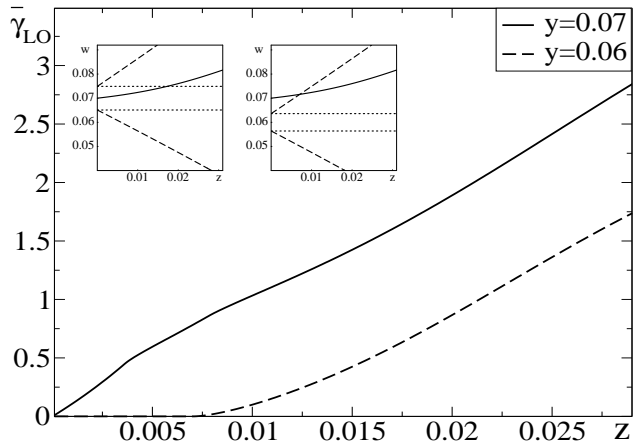


FIG. 3: SO-induced damping of the LO phonon $\bar{\gamma}_{LO}(z) = \gamma_{LO}(z) \times 10^4$ for $w_0 = 0.07$, $r_s = 0.4$, $\varepsilon_\infty = 12$ and $\varepsilon_0 = 15$. Solid and dashed lines correspond to the cases $y = 0.07$ ($|w_0 - y| < y^2$) and $y = 0.06$ ($|w_0 - y| > y^2$), respectively. Insets show the location of the phonon spectrum (solid line) relative to the SO-induced damping region (dashed lines) and to the strip $y - y^2 < w < y + y^2$ (dotted lines) for $y = 0.07$ (left) and $y = 0.06$ (right).

a number of new screening properties: the region of particle-hole excitations is extended, and the plasmon mode experiences additional broadening. The same mechanism leads to the generation of the SO-induced lifetime for the longitudinal optical phonons. Thus, spin-orbit coupling tends to suppress collective excitations. At the same time, it does not affect much the position of the collective mode dispersions. Comparison of our theoretical estimates for SO-induced lifetimes with the values obtained in the recent Raman scattering measurements suggests that the effects described here can be observed experimentally.

We are grateful to Dionys Baeriswyl, Gerd Schön and Emmanuel Rashba for valuable discussions. M.P. was supported by the DFG Center for Functional Nanostructures at the University of Karlsruhe. V.G. was supported by the Swiss National Science Foundation through grant Nr.20-68047.02.

-
- [1] T. Ando, A. Fowler, and F. Stern, *Rev. Mod. Phys.* **54**, 437 (1982).
 - [2] G. D. Mahan, *Many-Particle Physics*, Plenum Press, NY, 1990.
 - [3] F. Stern, *Phys. Rev. Lett.* **18**, 546 (1967).
 - [4] S. J. Allen, Jr., D. C. Tsui, and R. A. Logan, *Phys. Rev. Lett.* **38**, 980 (1977).
 - [5] T. Nagao *et al.*, *Phys. Rev. Lett.* **86**, 5747 (2001).
 - [6] C. F. Hirjibehedin *et al.*, *Phys. Rev. B* **65**, 161309 (2002).
 - [7] I.V. Kukushkin *et al.*, *Phys. Rev. Lett.* **90**, 156801 (2003).
 - [8] I. Žutić, J. Fabian, and S. Das Sarma, *Rev. Mod. Phys.* **76**, 323 (2004); R. H. Silsbee, *J. Phys.: Condens. Matter* **16**, R179 (2004).
 - [9] J. Nitta *et al.*, *Phys. Rev. Lett.* **78**, 1335 (1997); Y. Kato *et al.*, *Nature* **427**, 50 (2004).
 - [10] S. Murakami, N. Nagaosa, and S. C. Zhang, *Science* **301**, 1348 (2003); J. Sinova *et al.*, *Phys. Rev. Lett.* **92**, 126603 (2004).
 - [11] G.-H. Chen and M. E. Raikh, *Phys. Rev. B* **59**, 5090 (1999).
 - [12] Y.A. Bychkov and E.I. Rashba, *J. Phys. C* **17**, 6039 (1984).
 - [13] A. Czachor *et al.*, *Phys. Rev. B* **25**, 2144 (1982).
 - [14] L.I. Magarill, A.V. Chaplik, and M.V. Éntin, *JETP* **92**, 153 (2001).
 - [15] E. G. Mishchenko and B. I. Halperin, *Phys. Rev. B* **68**, 045317 (2003).
 - [16] D. S. Saraga and D. Loss, cond-mat/0504661.
 - [17] B. Jusserand *et al.*, *Phys. Rev. Lett.* **69**, 848 (1992).
 - [18] D. Grundler, *Phys. Rev. Lett.* **84**, 6074 (2000).
 - [19] S. D. Ganichev *et al.*, *Phys. Rev. Lett.* **92**, 256601 (2004).
 - [20] G. Engels *et al.*, *Phys. Rev. B* **55**, 1958 (1997).
 - [21] B. Jusserand *et al.*, *Phys. Rev. B* **63**, 161302 (2001).
 - [22] A. L. Fetter, *Phys. Rev. B* **10**, 3739 (1974).
 - [23] R. Jalabert and S. Das Sarma, *Phys. Rev. B* **40**, 9723 (1989).
 - [24] M. Canonico *et al.*, *Phys. Rev. Lett.* **88**, 215502 (2002).